Available online at www.sciencedirect.com

ScienceDirect

Ceramics International 42 (2016) 6761–6769

CERAMICS INTERNATIONAL

www.elsevier.com/locate/ceramint

Microstructure, optical, electrical properties, and leakage current transport mechanism of sol–gel-processed high-*k* HfO_2 gate dielectrics

Peng Jin[a], Gang He[a,*], Dongqi Xiao[a], Juan Gao[a], Mao Liu[b,*], Jianguo Lv[c,*], Yanmei Liu[a], Miao Zhang[a], Peihong Wang[a], Zhaoqi Sun[a]

[a]*School of Physics and Materials Science, Radiation Detection Materials & Devices Lab, Anhui University, Hefei 230601, China*
[b]*Key Laboratory of Materials Physics, Anhui Key Laboratory of Nanomaterials and Nanostructure, Institute of Solid State Physics, Chinese Academy of Sciences, Hefei 230031, China*
[c]*Department of Physics and Electronic Engineering, Hefei Normal University, Hefei 230061, China*

Received 1 January 2016; received in revised form 8 January 2016; accepted 8 January 2016
Available online 14 January 2016

Abstract

Deposition of high-*k* HfO_2 gate dielectric films on n-type Si and quartz substrates by sol–gel spin-on coating technique has been performed and the structural, optical and electrical characteristics as a function of annealing temperature have been investigated. The structural and optical properties of HfO_2 thin films related to annealing temperature are investigated by X-ray diffraction (XRD), ultraviolet–visible spectroscopy (UV–vis), and spectroscopic ellipsometry (SE). Results indicate that the monoclinic form of HfO_2 appears when temperature rises through and above 500 °C. The reduction in band gap is observed with the increase of annealing temperature. Moreover, the increase of refractive index (n) and density and the decrease of the extinction coefficient with the increase of annealing temperature are obtained by SE measurements. Additionally, the electrical properties based on Al/Si/HfO_2/Al capacitor are analyzed by means of the high frequency capacitance–voltage (C–V) and the leakage current density–voltage (J–V) characteristics. And the leakage current conduction mechanisms as functions of annealing temperatures are also discussed.

Keywords: High-*k* gate dielectrics; Sol–gel; Electrical properties; Leakage current transport mechanism; Optical properties

1. Introduction

HfO_2 thin film has been widely investigated as a potential high-*k* oxide in replacement of SiO_2 in future silicon microelectronics because of its excellent thermal, chemical stability, large band gap energy ($\sim$5.8 eV) and large band offsets relative to Si substrate [1–5]. By far, many methods have been carried out to prepare HfO_2 thin films, such as RF sputtering, atomic layer deposition (ALD), chemical vapor deposition (CVD), sol–gel and so on [6–11]. ALD is a good way to obtain gate dielectric for its better uniformity and coverage. It was shown by Liu et al. [12] that high quality HfO_2 films have been deposited on hydrogen-terminated diamond by ALD and show best electrical properties after annealing at 300 °C. But the ALD require a vacuum environment, and thin film growth rate is very low, that is not conducive to large-scale modern production. Traditional film preparation methods such as RF sputtering, CVD both need high vacuum environment. The vacuum equipment makes high productive cost in the process of thin films growth, and are not good for large area of modern production. However, the sol–gel processing has been widely used to fabricate high-quality ceramics and glasses with the advantages of low cost, relative simplicity, and easier control of the composition of the films [13]. Nowadays, many high-quality metal-oxide-semiconductor (MOS) and thin-film-transistor (TFT) devices were produced by sol–gel method because of low cost of this method. In current work, the fabrication of solution-processed high-*k* HfO_2 related with the annealing temperature has been described. Normally, $HfCl_4$ precursors are usually used with an alcohol solvent for

---

[*] Corresponding authors.

E-mail addresses: hegang@ahu.edu.cn (G. He), mliu@issp.ac.cn (M. Liu), jglv@hftc.edu.cn (J. Lv).

http://dx.doi.org/10.1016/j.ceramint.2016.01.050
0272-8842/

solution processing of HfO_2 thin films. In the decomposition process of $HfCl_4$, it transforms into Hafnium ethoxide and then decomposes into the final product of HfO_2 upon thermal annealing.

From the decomposition process, it can be noted that annealing temperature have great influence on the quality of HfO_2 thin film formation. And the density of the films fabricated by sol–gel method are not as enough large as that fabricated by RF sputtering and ALD. So the annealing temperature is an important affecting factor to improve the quality of thin film. By far, little related references have been reported on the effect of annealing temperature on the optical and electrical properties of sol–gel-derived HfO_2 gate dielectrics. In this paper, high-*k* gate dielectric HfO_2 thin films have been spin coated on Si substrate by sol–gel and the structural, optical and electrical properties of samples have been investigated at different annealing temperature. The microstructure of the HfO_2 thin films has been analyzed based on the analysis of XRD measurement. The thickness and optical constants of HfO_2 thin films have been discussed in detail through spectroscopic ellipsometry (SE) and ultraviolet-visible spectroscopy (UV–vis) measurements. Additionally, the high frequency capacitance–voltage (*C*–*V*) and the leakage current density–voltage (*J*–*V*) characteristics were analyzed systematically.

2. Experimental procedure

2.1. Preparation of the precursor solutions

The hafnium solution was prepared by dissolving hafnium chloride ($HfCl_4$, 99.9%, Aldrich) in ethanol (AR), followed by the addition of small amount of deionized water to a Hf concentration of 0.1 M. The solution was rigorously stirred for 2 h at room temperature, resulting in a transparent solution. And then the solution was filtered through a 0.2 mm membrane syringe filter.

2.2. Film deposition and characterization

Before the spin-coating, the n-type Si (100) substrates with resistivity of 2–5 Ω/cm were ultrasonically cleaned by ethanol for 10 min at room temperature, and then by a mixed solution ($NH_4OH:H_2O_2:H_2O=2:1:7$) for 10 min at 75 °C to remove organic matter and other impurity ions that had adhered to the surfaces of the substrates. And the substrates were cleaned in a hydrofluoric acid solution for 10 s to remove native oxides and form Si–H passivation layer on the Si surface. The substrates were ultrasonically cleaned with acetone and deionized water some times to ensure a hydrophilic surface before spin coating. The Hf solution was spin coated 5000 rpm for 30 s and the substrate was then placed on a hotplate to bake at 200 °C for 10 min to remove solvent residues. This procedure was repeated until the desired thickness was obtained. Finally, the substrate was placed on a oven and annealed at selected temperatures 400 °C, 500 °C and 600 °C for 1 h to complete the process. Fig. 1 shows the details of the HfO_2 thin film preparation method.

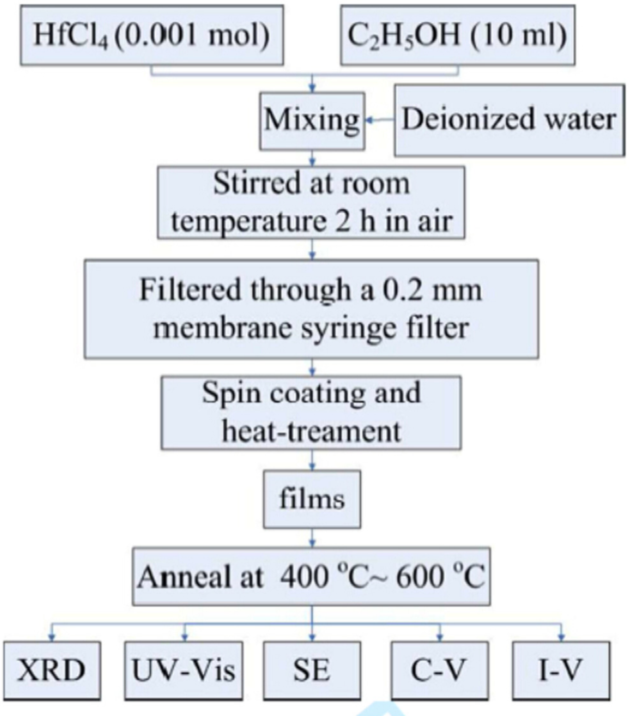

Fig. 1. The schematic flow chart of HfO_2 thin film by sol–gel method.

2.3. Metal insulator semiconductor (MIS) device fabrication and characterization

In order to fabricate MOS capacitors, Al gate electrode was deposited on the HfO_2 film by radio frequency magnetron sputtering through a shadow mask with an area of 7.065×10^{-4} cm^2. To explore the properties of the film, X-ray diffraction (XRD) has been used to analyze the microstructure and crystallization of the films. The ultraviolet visible spectroscopy (UV–vis) was used to measure the band gap and transmittance spectra of the films. Spectroscopy ellipsometry (SE) has been carried out to obtain the thickness and optical constant of the HfO_2 thin films. The high frequency capacitance–voltage (*C*–*V*) measurements were performed using a semiconductor device analyzer (Agilent B1500A) combined with Cascade Probe Station at 1 MHz. And the leakage current density–voltage (*J*–*V*) characteristics were measured by B1500A. All the electrical characterization was performed at room temperature in a shielded dark box.

3. Result and discussion

3.1. X-ray diffraction analysis

The microstructures of the HfO_2 thin films are analyzed based on the analysis of the XRD spectrum shown in Fig. 2. From Fig. 2, no distinguishable diffraction peaks are observed for films annealed at temperatures lower than 400 °C for 1 h. As the temperature rises through and above 500 °C, the monoclinic form of HfO_2 films appears. It is well known that an amorphous phase of HfO_2 thin film is stable under 500 °C

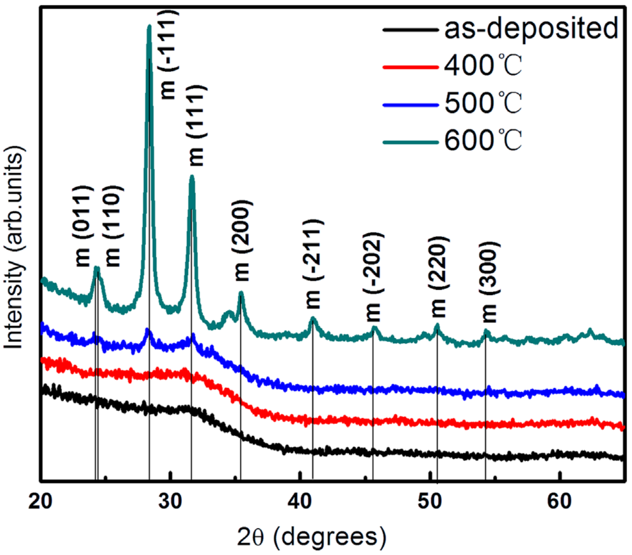

Fig. 2. XRD spectra of HfO_2 thin films as a function of annealing temperature.

[14,15], which is consistent with our current results. For crystallized high *k* dielectric materials, the grain clearance can be used as a current channel, resulting in the increase of leakage current, and grain clearance also strengthens the diffusion of impurity atoms [16], which seriously affects the performance and reliability of the device. As a result, amorphous high-*k* dielectric materials will have a good application in CMOS and thin film transistor.

3.2. Ultraviolet visible spectroscopy (UV–vis) analysis

The annealed temperature dependent optical absorption and transmittance spectra of HfO_2 thin films were performed by ultraviolet-visible spectroscope. Fig. 3 shows the transmittance spectra of HfO_2 thin films coated on quartz substrate in the wavelength ranging of 190–900 nm. Average transmission of all the HfO_2 samples are about 80% owing to their uniform composition as well as the film deposited by ALD [7].

The absorption spectra of the HfO_2 thin films deposited at different annealing temperature are shown in Fig. 4. It is known that HfO_2 is indirect band gap insulator [17], so the energy band gap (E_g) value of the HfO_2 film is obtained by absorption spectra and plotting $(\alpha h\upsilon)^{1/2}$ vs photon energy ($h\upsilon$) using the following relation [18,19]:

$$(\alpha h\upsilon)^{1/2} = A(h\upsilon - E_g) \quad (1)$$

where α, $h\upsilon$, A and E_g is absorption coefficient, photon energy, constant and optical band gap energy of HfO_2 thin film, respectively. Fig. 4 shows the $(\alpha h\upsilon)^{1/2}$ versus photon energy ($h\upsilon$) curves near the band edge of all the films, and the values of E_g are estimated by leading to a tangent of the curves relating $(\alpha h\upsilon)^{1/2}$ and ($h\upsilon$) to $h\upsilon$ axis to determine the energy band gap. It can be concluded that the band gap of the HfO_2 film decreases from 5.60 to 5.13 eV with increasing annealing temperature. The reduction in band gap as a function of annealing temperature can be attributed to the evolution of the microstructure from amorphous to crystallized state and the increase in HfO_2 grain size after annealing, which agrees with the results of Deng et al. [6].

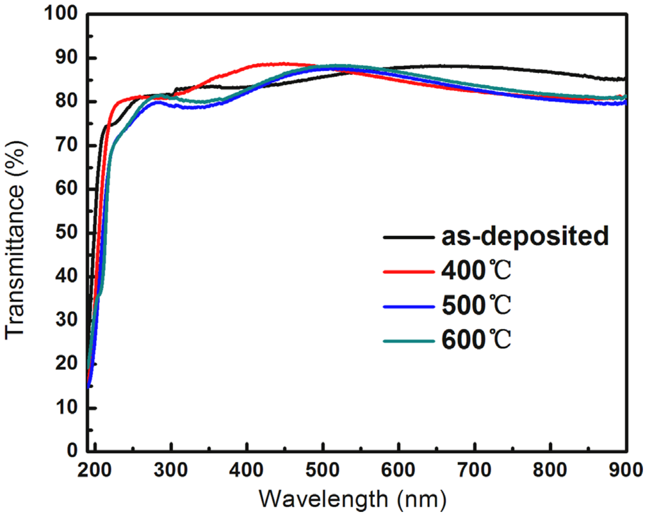

Fig. 3. Transmission spectra of HfO_2 thin films.

3.3. Spectroscopic ellipsometry analysis

The SE was used to measure annealing temperature dependent optical functions of HfO_2 thin films at room temperature in the spectral range of 190–900 nm. Dispersion curves are well represented by the Cauchy formula. The thickness of HfO_2 thin films obtained from the fitting results with the as-deposited and annealing temperature of 400, 500 and 600 °C is shown in Table 1. The fitting results of the refractive index $n(\lambda)$ for as-deposited, 400, 500, and 600 °C annealed films are shown in Fig. 5. The n is given by following equations as a function of the wavelength [20],

$$n(\lambda) = A_n + B_n/\lambda^2 + C_n/\lambda^4 \quad (2)$$

where A_n, B_n, C_n (index parameters which specify the index of refraction) are defined variable fit parameters during the data fitting. Fig. 5 shows the dispersion relation of refractive index n of HfO_2 thin films with the different annealing temperature. There is an obvious increase in the value of refractive index with increasing annealing temperature. It agrees with the results of Jiang et al. [21]. It is well known that the refractive index is closely related to the density of materials [22]. By the analysis as follow, the density of HfO_2 thin films increase with increase of annealing temperature. So the higher annealing temperature, the higher refractive index has been obtained for HfO_2 thin films.

From Fig. 5, the refractive index of the HfO_2 thin films are in the range of 1.81–1.97 at wavelength of 550 nm, which is comparable to vacuum-deposited thin films. From the variation of thickness and refractive index, it represents the evolution of the packing density of HfO_2 thin film related with the annealing temperature. With the refractive index values at 550 nm wavelength, the density of the HfO_2 thin film could be calculated with the following formula [23]:

$$\rho = 11.36n - 14.43 \quad (3)$$

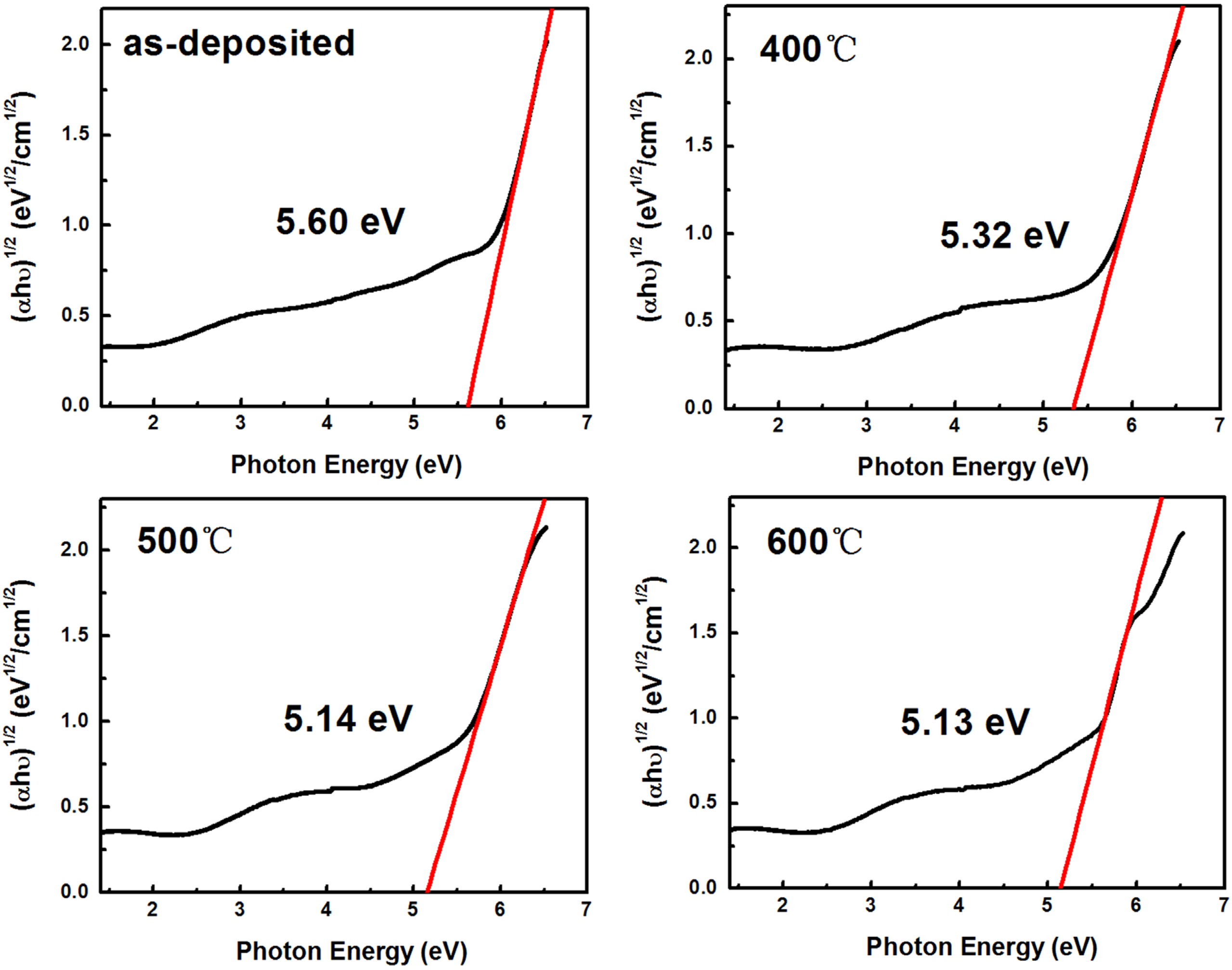

Fig. 4. Band gap values determined by optical method using $(\alpha h\upsilon)^{1/2} \sim h\upsilon$ plots of HfO_2 films deposited on quartz substrate.

Table 1
Model fitting results for the thickness of HfO_2 and their refractive indices.

Annealing temperature(°C)	Thickness (nm)	refractive index at $\lambda = 550$ nm	Density (g/cm^3)
As-deposited	95.99	1.81	6.13
400	80.89	1.85	6.58
500	80.93	1.93	7.49
600	75.82	1.97	7.95

From Table 1, the densities of the HfO_2 thin films increase from 6.13 g/cm^3 to 7.95 g/cm^3 with increase of annealing temperature. But this value is lower than the theoretical value of 9.68 g/cm^3 [24]. The oxide films fabricated by sol–gel method generally have density lower than the vacuum-deposited films.

3.4. Electrical properties analysis

To investigate the annealing temperature dependence on the electrical properties of HfO_2 thin films, capacitors with Al electrodes with the area of 7.065×10^{-4} cm^2 through a shadow mask were fabricated. Through the measurement of the SE, the thicknesses of the HfO_2 thin films are 20.78, 16.36, 16.31 and 14.57 nm at as-deposited, 400, 500 and 600 °C, respectively. High frequency (1 MHz) *C*–*V* characteristics

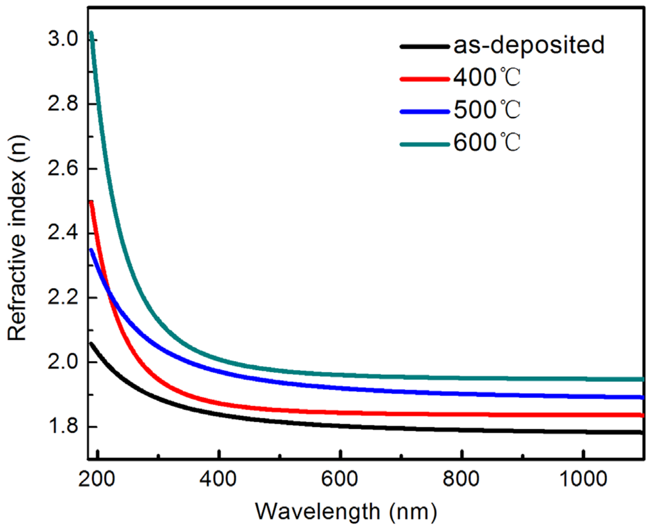

Fig. 5. The calculated refractive index *n* dispersion relation of the HfO_2 films derived from the results of the Cauchy fitting.

curves for as-deposited and annealed HfO_2 gate dielectric MOS capacitors are presented in Fig. 6 and the dielectric constants are calculated and shown in Table 2. In order to analyze electrical properties of the HfO_2 thin films better, the equivalent oxide thickness (E_{ot}), dielectric constant (k), flat-band capacitance (C_{fb}), flat-band voltage (V_{fb}) and hysteresis ($\Delta V_{Hysteresis}$) of samples will been analyzed. The equivalent oxide thickness can be obtained by following relation [25]:

$$E_{ot} = \frac{K_{SiO_2} \epsilon_0 A}{C_{ox}} \tag{4}$$

where the K_{SiO2} is the dielectric constant of SiO_2 with the value of 3.9, A is the area of Al electrodes. From Table 2, the smallest equivalent oxide thickness is 3.10 nm when the annealing temperature is 400 °C. According to the equivalent oxide thickness, the dielectric constant k of HfO_2 thin films through the equation can be derived [1]:

$$K_{high-k} = \frac{K_{SiO_2} \times t_{high-k}}{E_{ot}} \tag{5}$$

The $t_{high\text{-}k}$ is the thickness of HfO_2 thin films. The dielectric constant k of samples is shown in Table 2. From the Table 2, the biggest dielectric constant k is 20.58 at 400 °C. The value is larger than the value of the film deposited by ALD [7]. For the amorphous HfO_2 thin films, high annealing temperature can inhibit the oxygen diffusion, which can restrain the growth of the interface layer and attribute the increase of dielectric constant. When the annealing temperature rises through 500 °C, film grain clearance leads to the increased oxygen diffusion and reduced dielectric constant. With the increase of the annealing temperature, film crystallization degree increase, which enhances film's ability of store electric charge and the dielectric constant.

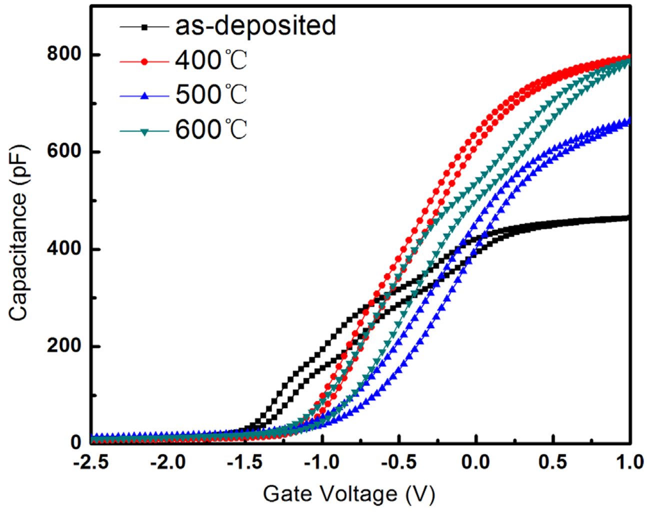

Fig. 6. Annealing temperature-dependent C–V characteristics of HfO_2 gate dielectric MOS capacitors.

The flat band capacitance (C_{fb}) is obtained by using the following relation [25]:

$$C_{fb} = \frac{C_{ox}}{1 + \frac{\epsilon_{ro}}{\epsilon_{rs} d_{ox}} \sqrt{\frac{kT\epsilon_0 \epsilon_{rs}}{q^2 N_A}}} \tag{6}$$

where ϵ_{ro} is the dielectric constant of the HfO_2 film, ϵ_{rs} is the dielectric constant of the Si substrate, N_A is the carrier concentration and d_{ox} is the thickness of the film. The flat band voltage (V_{fb}) values can be obtained through the C_{fb} values from C–V curve [26]. The V_{fb} and C_{fb} values are shown in Table 2. From Table 2, the negative V_{fb} of HfO_2 films are shown with the change of the annealing temperature. From Fig. 6 and Table 2, it can be clearly seen that HfO_2 thin films annealed at 400 °C demonstrate smaller hysteresis. The hysteresis is related to border trapped oxide charge density indicating that the sample annealed at 400 °C has smaller border trapped oxide charge density [27].

The I–V characteristics of HfO_2 gate dielectric MOS capacitors are demonstrated in Fig. 7. The lowest leakage current density 2.5×10^{-4} A/cm^2 at the gate voltage of 2 V is observed for HfO_2 thin film annealed at 400 °C and 500 °C. The leakage current density is similar to the results showed by Gao et al. [28] in the case of thinner thin film. The increase of the annealing temperature makes the surface of sample becomes denser and the film has better surface adhesion, inducing the effectively suppressed interface-state density and traps. However, the monoclinic form of HfO_2 film appears and leakage current density begin to increase when the annealing temperature rises through and above 500 °C. For polycrystalline high k dielectric materials, the grain clearance can be used as a current channel, resulting in leakage current increase, and grain clearance also strengthens the diffusion of impurity atoms [17]. The results demonstrate that HfO_2 thin film annealed at 400 °C shows the optimized electrical properties.

3.5. Leakage current mechanism analysis

In order to further understand the carrier transportation mechanisms of the HfO_2/n-Si gate stacks, the leakage current conduction mechanism was investigated. The gate voltage is

Table 2
Gate-oxide capacitance (C_{ox}), equivalent oxide thickness (E_{ot}), dielectric constant (k), flat-band capacitance (C_{fb}), flat-band voltage (V_{fb}) and hysteresis ($\Delta V_{Hysteresis}$) of samples extracted from 1MHz C–V curves.

Annealing temperature (°C)	**C_{ox} (pF)**	**E_{ot} (nm)**	**k**	**C_{fb} (pF)**	**V_{fb} (V)**	**$\Delta V_{Hysteresis}$ (V)**
As-deposited	**446.21**	**5.46**	**14.84**	**111.55**	**−1.15**	**0.10**
400	**785.99**	**3.10**	**20.58**	**105.93**	**−0.97**	**0.06**
500	**649.18**	**3.76**	**16.92**	**110.22**	**−0.76**	**0.14**
600	**773.46**	**3.14**	**18.10**	**105.95**	**−0.95**	**0.17**

positive (substrate injection) for the n-substrate capacitors, while negative (gate injection) for the p-substrate samples [29]. Several typical leakage current conduction mechanisms of the HfO_2/n-Si stacks at different deposition temperatures are showed from Figs. 8–11. For the substrate injection (positive voltage on the Al electrode), Figs. 8(a) and 10(a) plot J versus E in low electric filed ($E < 0.8$ MV/cm), and the linear trend of ohmic conduction indicates Al top electrodes have a good contact with as-deposited HfO_2 thin film and thin film annealed at 500 °C.

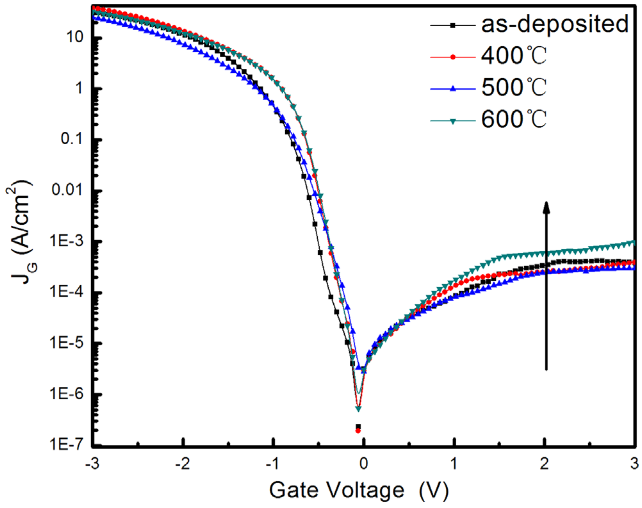

Fig. 7. Annealing temperature-dependent J–V characteristics of HfO_2 gate dielectric MOS capacitors.

While with electric field increases, $\ln(J/T^2)$ versus the $E^{1/2}$ is plotted shown in Fig. 8(b), Fig. 9(b), Fig. 10(b) and Fig. 11(b), respectively. A good linear fitting indicate the main current conduction mechanisms is Schottky emission [27]. The standard Schottky emission can be expressed as [30]

$$J = A^{*}T^{2}\exp\left[\frac{-q(\phi_B - \sqrt{qE/4\pi\epsilon_r\epsilon_0})}{kT}\right] \tag{7}$$

where $A^{*}=4\pi q(m^{*}_{ox})k^2/h^3=120(m^{*}_{ox}/m_0)$ (A/cm^2 K^2), J is the current density, A^* is the effective Richardson constant, T is the absolute temperature, q is the electronic charge, $q\phi_B$ is the Schottky barrier height ($\Phi_B = q\phi_B$), E is the electric field, k is Boltzmann's constant, h is Planck's constant, ε_0 is the permitivity of free space, ε_r is the dynamic dielectric constant, m_0 is the free electron mass, and m^{*}_{ox} is the electron effective mass in HfO_2. The slope of the curves is deduced from Schottky emission expression as follows:

$$\text{slope} = \frac{1}{kT}\sqrt{\frac{q^3}{4\pi\epsilon_0\epsilon_r}} \tag{8}$$

from which the dielectric constant (ε_r) of HfO_2 films can be calculate. The dielectric constant (ε_r) of HfO_2 films with as-

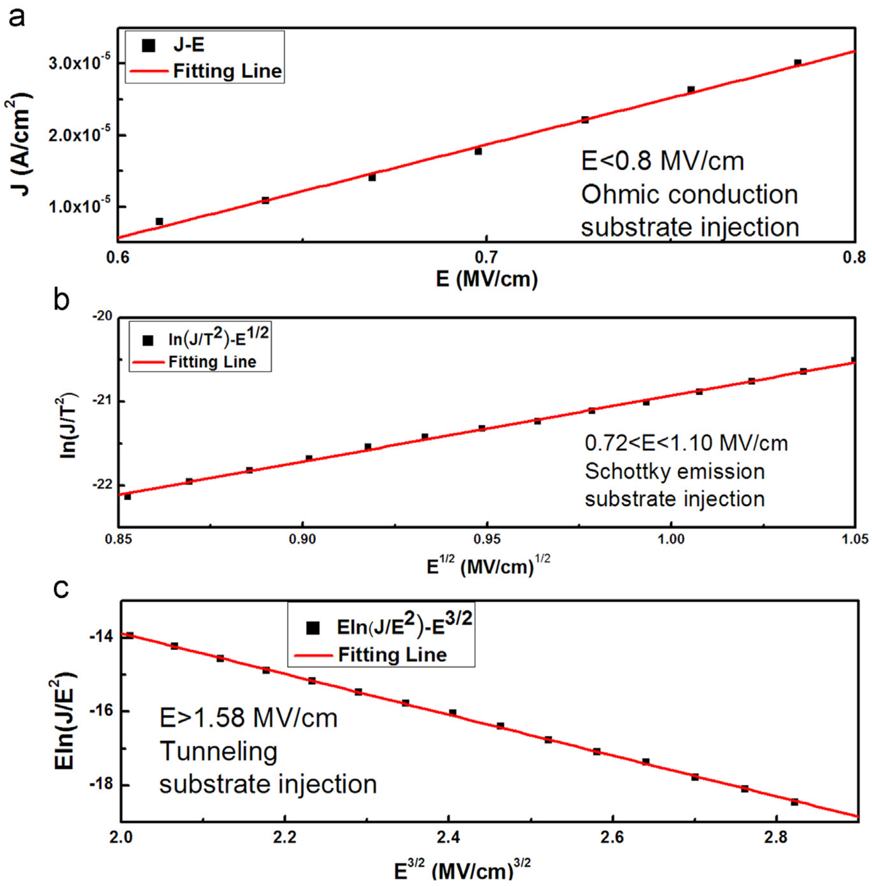

Fig. 8. Conduction mechanism fitting of as-deposited HfO_2 thin film under substrate injection. (a) The curve of J vs E in low electric field ($E < 0.8$ MV/cm); (b) the curve of $\ln(J/T^2)$ vs $E^{1/2}$ in moderate electric field ($0.72 < E < 1.10$ MV/cm); (c) the curve of $E\ln(J/E^2)$ vs $E^{3/2}$ in high electric field ($E > 1.58$ MV/cm).

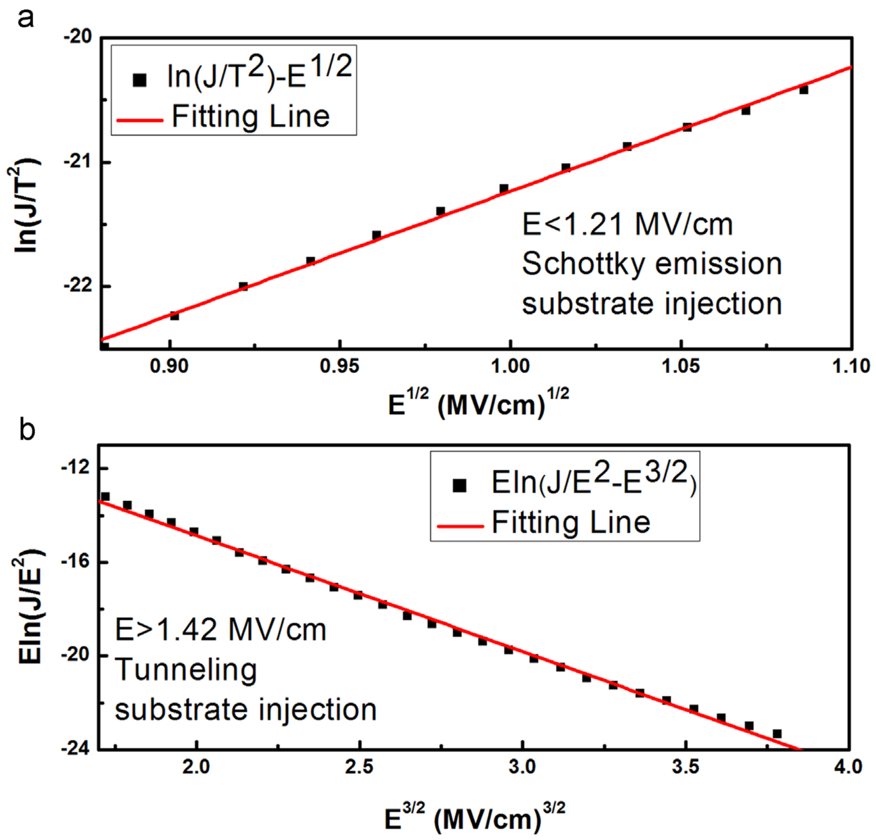

Fig. 9. Conduction mechanism fitting of HfO_2 thin film deposited at 400 °C under substrate injection. (a) The curve of $\ln(J/T^2)$ vs $E^{1/2}$ in low electric field ($E < 1.21$ MV/cm); (b) the curve of $E\ln(J/E^2)$ vs $E^{3/2}$ in high electric field ($E > 1.42$ MV/cm).

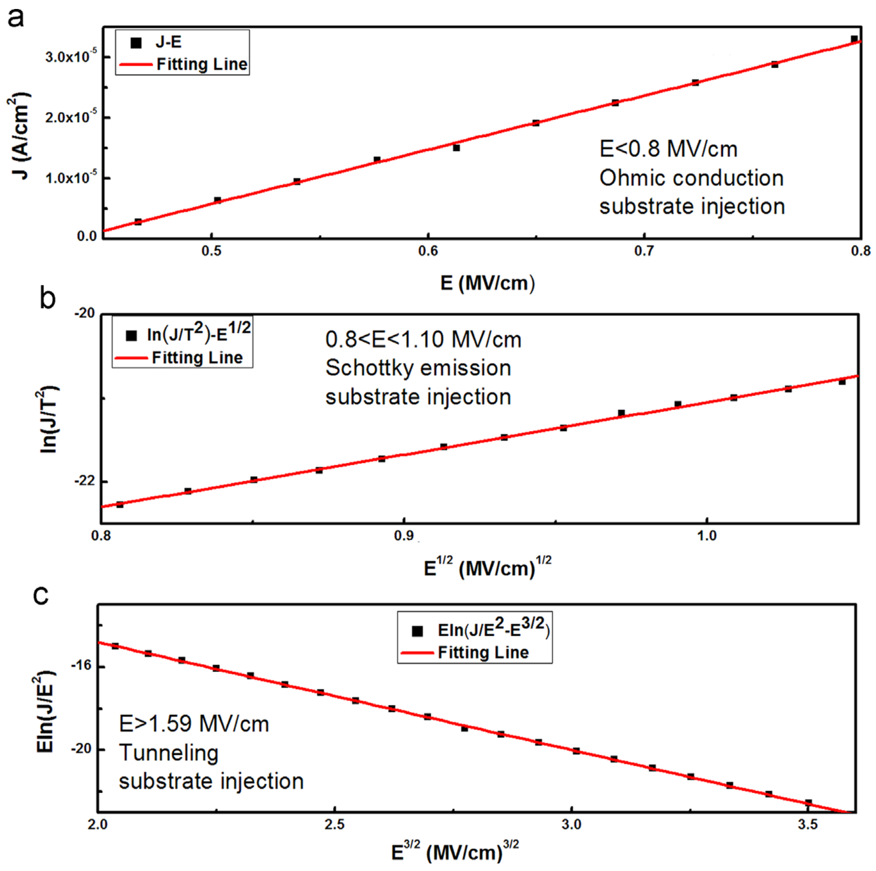

Fig. 10. Conduction mechanism fitting of HfO_2 thin film deposited at 500 °C under substrate injection. (a) The curve of J vs E in low electric field ($E < 0.8$ MV/cm); (b) the curve of $\ln(J/T^2)$ vs $E^{1/2}$ in moderate electric field ($0.80 < E < 1.10$ MV/cm); (c) the curve of $E\ln(J/E^2)$ vs $E^{3/2}$ in high electric field ($E > 1.59$ MV/cm).

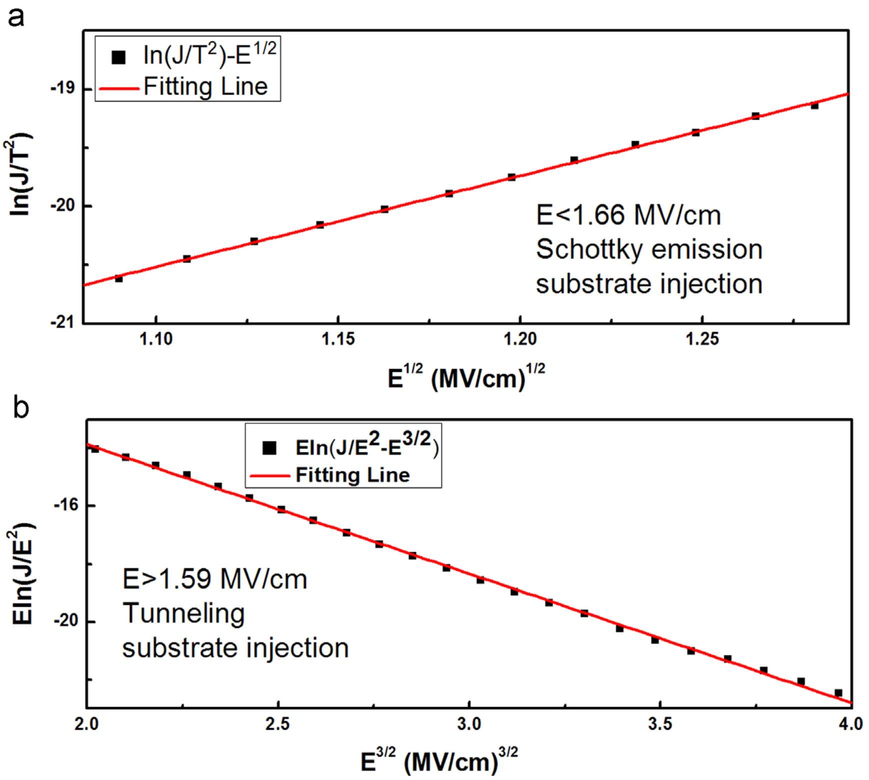

Fig. 11. Conduction mechanism fitting of HfO_2 thin film deposited at 600 °C under substrate injection. (a) The curve of $\ln(J/T^2)$ vs $E^{1/2}$ in low electric field ($E < 1.66$ MV/cm); (b) the curve of $E\ln(J/E^2)$ vs $E^{3/2}$ in high electric field ($E > 1.59$ MV/cm).

deposited, annealed at 400 °C, 500 °C and 600 °C are close to 3.62, which is the square of the refractive index $n = \varepsilon_r^{1/2} = 1.90$, 1.48, 2.38 and 1.92 [31]. The intercept of the Schottky plot with the vertical axis can be expressed as [32]

$$\text{Intercept} = \ln(A^*) - \frac{q\phi_B}{kT},\; A^* = 120\frac{m^*_{ox}}{m_0} \qquad (9)$$

from which the extracted Schottky barrier height between Al and HfO_2 with as-deposited, annealed at 400 °C, 500 °C and 600 °C are about 0.80 eV, 0.87 eV, 0.77 eV and 0.81 eV, respectively. As the applied electric field further increases, the conduction mechanisms of HfO_2 films with as-deposited, annealed at 400 °C, 500 °C and 600 °C convert into direct tunneling. The linear fitting graphs of $E\ln(J/E^2)$ versus $E^{3/2}$ are respectively given in Fig. 8(c), Fig. 9(c), Fig. 10(c) and Fig. 11 (c). It can clearly seen that data fittings of direct tunneling are presented in high electric field of $E > 1.58$ MV/cm for as-deposited and $E > 1.42$, 1.59, 1.59 MV/cm for HfO_2 thin films annealed at 400 °C, 500 °C, and 600 °C.

4. Conclusions

In current study, annealing temperature dependent optical and electrical properties of sol–gel spin-on coating HfO_2/n-Si gate stacks have been systematically investigated. XRD analysis shows that the films keeps amorphous state until annealing temperature achieves 500 °C. By UV–vis analysis, average transmission of all the HfO_2 samples is about 80%. The red shift in band gap has been observed by UV–vis measurement. By SE measurement, the thickness and density of the films are obtained by fitting the experimental spectroscopic ψ and Δ with Cauchy–Urbach dispersion model. The density and refractive index of the films increase with increase annealing temperature. Through electrical properties analysis, the highest k value of the HfO_2 film annealed at 400 °C is observed. However, the lowest leakage current density is observed for HfO_2 thin film at 400 °C and 500 °C. On the whole, the HfO_2 thin film annealed at 400 °C displays excellent performance as promising candidates for future high-k gate dielectrics. The analysis of conduction mechanism fitting for HfO_2 thin films is summarized as follows: the dominant conduction mechanisms is Ohmic conduction under substrate injection for as-deposited HfO_2 thin film and thin film annealed at 500 °C at low electrical field; at moderate electrical field, the main current conduction mechanisms is Schottky emission under substrate injection for all thin films. And it changes into direct tunneling under substrate injection for all thin films at high electrical field.

Acknowledgments

The authors acknowledge the support from National Key Project of Fundamental Research (2013CB632705), National Natural Science Foundation of China (51572002, 11474284 and 51472003), Technology Foundation for Selected Overseas Chinese Scholar, Ministry of Personnel of China (J05015131), Anhui Provincial Natural Science Foundation (1608085MA06), Outstanding Young Scientific Foundation and Youth Science

Research Foundation of Anhui University (KJJQ1103), and “211 project” of Anhui University.

References

[1] G.D. Wilk, R.M. Wallace, J.M. Anthony, High-*k* gate dielectrics: current status and materials properties considerations, J. Appl. Phys. 89 (2001) 5243–5275.

[2] G. He, B. Deng, M. Liu, Y.Q. Ma, X.S. Chen, J.G. Lv, S.W. Shi, X.P. Song, Z.Q. Sun, Oxynitridization dependent interface control and band alignment of AlON/SiON/Si gate stacks grown by metalorganic chemical vapor deposition, Sci. Adv. Mater. 5 (6) (2013) 709–712.

[3] H. Sim, H. Hwang, Effect of deuterium postmetal annealing on the reliability characteristics of an atomic-layer-deposited HfO_2/SiO_2 stack gate dielectrics, Appl. Phys. Lett. 81 (21) (2002) 4038–4040.

[4] H. Lee, S. Jeon, H. Hwang, Electrical characteristics of a Dy-doped HfO_2 gate dielectric, Appl. Phys. Lett. 79 (16) (2001) 2615–2617.

[5] G. He, Q. Fang, M. Liu, L.Q. Zhu, L.D. Zhang, The structural and interfacial properties of HfO_2/Si by the plasma oxidation of sputtered metallic Hf thin films, J. Cryst. Growth. 268 (1–2) (2004) 155–162.

[6] B. Deng, G. He, X.S. Chen, X.F. Chen, J.W. Zhang, M. Liu, J.G. Lv, Z.Q. Sun, Annealing temperature dependence on the structural and optical properties of sputtering-grown HfO_2 high-*k* gate dielectrics, J. Mater. Sci.: Mater. Electron. 25 (9) (2014) 4163–4169.

[7] J. Gao, G. He, J.W. Zhang, Y.M. Liu, Z.Q. Sun, Deposition temperature dependent optical and electrical properties of ALD HfO_2 gate dielectrics pretreated with Tetrakisethylmethylamino Hafnium, Mater. Res. Bull. 70 (2015) 840–846.

[8] J.W. Liu, M.Y. Liao, M. Imura, Y. Koide, Normally-off HfO_2-gated diamond field effect transistors, Appl. Phys. Lett. 103 (2013) 092905-1–092905-4.

[9] J.W. Liu, M.Y. Liao, M. Imura, Y. Koide, Band offsets Al_2O_3 and HfO_2 oxides deposited by atomic layer deposition technique on hydrogenated diamond, Appl. Phys. Lett. 101 (2012) 252108-1–252108-4.

[10] G. Lupina, M. Lukosius, J. Kitzmann, J. Dabrowski, A. Wolff, W. Mehr, Nucleation and growth of HfO_2 layers on graphene by chemical vapor deposition, Appl. Phys. Lett. 103 (18) (2013) 183116-1–183116-4.

[11] T. Nishide, S. Honda, M. Matsuura, M. Ide, Surface, structural and optical properties of sol–gel derived HfO_2 films, Thin Solid Films. 371 (1) (2000) 61–65.

[12] J.W. Liu, M.Y. Liao, M. Imura, H. Oosato, E. Watanabe, Y. Koide, Electrical characteristics of hydrogen-terminated diamond metal-oxide-semiconductor with atomic layer deposited HfO_2 as gate dielectric, Appl. Phys. Lett. 102 (2013) 112910-1–112910-4.

[13] J.J. Yu, Q. Fang, J.Y. Zhang, Z.M. Wang, I.W. Boyd, Hafnium oxide layers derived by photo-assisted sol–gel processing, Appl. Surf. Sci. 208–209 (2003) 676–681.

[14] S.V. Ushakov, A. Navrotsky, Y. Yang, S. Stemmer, K. Kukli3, M. Ritala, M.A. Leskelä, P. Fejes, A. Demkov, C. Wang, B.-Y. Nguyen, D. Triyoso, P. Tobin, Crystallization in hafnia- and zirconia- based systems, Phys. Status Solidi B 241 (10) (2004) 2268–2278.

[15] Z.J. Wang, T. Humagai, H. Kokawa, J. Tsuaur, M. Ichiki, R. Maeda, Crystalline phases, microstructures and electrical properties of hafnium oxide films deposited by sol–gel method, J. Cryst. Growth 281 (2005) 452–457.

[16] D. Patel, M. Patel, Leakage current reduction techniques for CMOS circuits, Int. J. Eng. Sci. 3 (2) (2014) 1363–1366.

[17] J.W. Zhang, G. He, J. Gao, X.S. Chen, X.F. Chen, B. Deng, Y.M. Liu, M. Zhang, J.G. Lv, Z.Q. Sun, Annealing temperature dependent microstructure and optical properties of HfxTi$_{1-x}$O$_2$ thin films, Sci. Adv. Mater. 6 (2014) 1–7.

[18] T.T. Tan, Zh.T. Liu, H. Ch., Lu, W.T. Liu, F. Yan, W.H. Zhang, Band structure and valence-band offset of HfO_2 thin film on Si substrate from photoemission spectroscopy, Appl. Phys. A 97 (2) (2009) 475–479.

[19] R. Ananthakumar, J.K. Sang, Synthesis and characterization of HfO_2 nanoparticles by sonochemical approach, J. Alloy. Compd. 544 (2012) 115–119.

[20] B. Farkas, J. Budai, P. Heszler, Zs Geretavszky, Optical characterization of PLD grown nitrogen-doped TiO_2 thin films, Appl. Surf. Sci. 254 (11) (2008) 3484–3488.

[21] K. Jiang, J.T. Anderson, K. Hoshino, D. Li, J.F. Wager, D.A. Keszler, Low-energy path to dense HfO_2 thin films with aqueous precursor, Chem. Mater. 23 (2011) 945–952.

[22] R. Hong, J. Huang, H. He, Z. Fan, J. Shao, Influence of different post-treatments on the structure and optical properties of zinc oxide thin films, Appl. Surf. Sci. 242 (3) (2005) 346–352.

[23] M. Jerman, Z. Qiao, D. Mergel, Refractive index of thin films of SiO_2, ZrO_2, and HfO_2 as a function of the films' mass density, Appl. Opt. 44 (15) (2005) 3006–3012.

[24] Y.B. Yoo, J.H. Park, K.H. Lee, H.W. Lee, K.M. Song, S.J. Lee, H. K. Baik, Solution-processed high-*k* HfO_2 gate dielectric processed under softening temperature of polymer substrates, J. Mater. Chem. C 1 (8) (2013) 1651–1658.

[25] J.B. Fan, H.X. Liu, Q.W. Kuang, B. Gao, F. Ma, Y. Hao, Physical properties and electrical characteristics of H_2O-based and O_3-based HfO_2 films deposited by ALD, Microelectron. Reliab. 52 (6) (2012) 1043–1049.

[26] H.X. Liu, Q.W. Kuang, S.Zh Luan, A. Zhao, Tallavarjula Sai, Frequency dispersion effect and parameters extraction method for novel HfO_2 as gate dielectric, Sci. China: Inf. Sci 53 (4) (2010) 878–884.

[27] J.Q. Zhang, Zh.X. Li, H. Zhou, C. Ye, H. Wang, Electrical, optical and micro-structural properties of ultra-thin HfTiON films, Appl. Surf. Sci. 294 (5) (2014) 58–65.

[28] J. Gao, G. He, B. Deng, D.Q. Xiao, M. Liu, P. Jin, C.Y. Zheng, Z.Q. Sun, Microstructure, wettability, optical and electrical properties of HfO2 thin film: effect of oxygen partial pressure, J. Alloy. Compd. 662 (2016) 339–347.

[29] Zh. Xu, M. Houssa, S.D. Gendt, M. Heyns, Polarity effect on the temperature dependence of leakage current through HfO_2/SiO_2 gate dielectric stacks, Appl. Phys. Lett. 80 (11) (2002) 1975–1977.

[30] K.C. Lin, J.Y. Chen, H.W. Hsu, H.W. Chen, C.H. Liu, Leakage current conduction behaviors of 0.65 nm equivalent-oxide-thickness HfZrLaO gate dielectrics, Solid-State Electron. 77 (2012) 7–11.

[31] F.C. Chiu, C.M. Lai, Optical and electrical characterizations of cerium oxide thin films, J. Phys. D.: Appl. Phys. 43 (7) (2010) 75104–75108 (5).

[32] F.C. Chiu, Interface characterization and carrier transportation in metal/HfO_2/silicon structure, J. Appl. Phys. 100 (11) (2006) 114102-1–114102-5.